Photodissociation of Acrylic Acid in the Gas Phase: An ab Initio Study

Wei-Hai Fang* and Ruo-Zhuang Liu

Contribution from the Department of Chemistry, Beijing Normal University, Beijing 100875, P. R. China

Received February 7, 2000. Revised Manuscript Received July 5, 2000

Abstract: The potential energy profiles, governing the dissociation of acrylic acid ($CH_2CHCOOH$) to $CH_3CH + CO_2$, $CH_2CHOH + CO$, $CH_2CH + COOH$ and $CH_2CHCO + OH$ in the ground as well as in the excited singlet and triplet states, have been determined using different ab initio quantum chemical methods with a correlation-consistent atomic natural orbital basis set of cc-pVDZ. The most probable mechanism leading to different products is characterized on the basis of the obtained potential energy surfaces of the dissociation and the crossing points of the surfaces.

1. Introduction

Ab initio methods have been very successful in studying ground-state reactivity of molecules. Experimental data can be reproduced well. In some case, deviations in the experimentally inferred structural parameters and thermodynamic properties were corrected by high-level theoretical calculations.[1−4] The characterization of photochemical reactions requires a knowledge of more than one potential energy surface (PES), including reaction pathways on different surfaces and the intersection region where the system decays from one state to another. In comparison with thermochemical reactions, photochemical reactions are difficult to treat computationally. However, molecular photochemistry has long been regarded as an important area of chemical physics, the results of which are relevant to atmospheric chemistry (especially the chemistry of planetary atmospheres), biological systems (enzymes, genes, and antibodies), and many other processes.[5−7] The number of ab initio studies of photochemical reactions has grown considerably during the last 10 years.[8−16]

α,β-unsaturated aldehydes and carboxylic acids can undergo a variety of photochemical processes, α-cleavage of the >C═O group, cycloadditions of the C═C chromophore, cis−trans isomerizations, and ring closure involving the C═C−C═O moiety. The photochemistry of these unsaturated compounds has been the subject of numerous experimental investigations.[17−34] An extensive CASSCF study[15] of the acrolein (CH_2CHCHO) was performed by Robb, Olivucci, and co-workers in order to provide a model for understanding the photoisomerization of the C═C−C═O moiety in α,β-enones. We have carried out ab initio calculations on the CH_2CHCHO photodissociation,[16] including decarbonylation, the C−C and C−H cleavages. Acrylic acid ($CH_2CHCOOH$) is one of the smallest α,β-unsaturated carboxylic acids, and it is an ideal system for investigating mechanismic photochemistry of this kind of molecules. As a series of work devoted to photochemistry of medium-size molecules, the $CH_2CHCOOH$ photodissociation is theoretically investigated in the present work.

In addition to early pyrolysis studies[29] of acrylic acid in the gas phase, a few recent experimental studies[30−37] concentrated

(1) Wesolowski, S. S.; Johnson, E. M.; Leininger, M. L.; Schaefer, H. F., III. *J. Chem. Phys.* **1998**, *109*, 2694−2699.
(2) Fang, W. H.; You, X. Z.; Zhi, Y. *Chem. Phys. Lett.* **1995**, *233*, 237−242.
(3) East, A. L. L.; Johnson, C. S.; Allen, W. D. *J. Chem. Phys.* **1993**, *98*, 1299.
(4) Skokov, S.; Peterson, K. A.; Bowman, J. M. *J. Chem. Phys.* **1988**, *109*, 2662.
(5) Rowland, F. S. *Annu. Rev. Phys. Chem.* **1991**, *42*, 731.
(6) Bortolus, P.; Monti, S. *Adv. Photochem.* **1995**, *21*, 218.
(7) Schinke, R. *Annu. Rev. Phys. Chem.* **1988**, *39*, 39.
(8) (a) Goldfield, E. M.; Gray, S. K.; Harding, L. B. *J Chem. Phys.* **1993**, *99*, 5812. (b) Loettgers, A.; Untch, A.; Keller, H.-M.; Schinke, R.; Werner, H.-J.; Bauer, C.; Rosmus, P *J. Chem. Phys.* **1996**, *106*, 3186.
(9) Yamaguchi, Y.; Wesolowski, S. S.; Van Huis T. J.; Schaefer H. F. *J. Chem. Phys.* **1998**, *108*, 5281 and references therein.
(10) Cotting, R.; Huber, J. R. *J. Chem. Phys.* **1996**, *104*, 6208.
(11) (a) Fang, W. H. *J. Am. Chem. Soc.* **1998**, *120*, 7568. (b) Fang. W. H.; You, X.-Z.; Yin, Z. *Chem. Phys. Lett.* **1995**, *238*, 236.
(12) Dunn, K. M.; Morokuma, K. *J. Phys. Chem.* **1996**, *100*, 123. (b) Cui. Q.; Morokuma, K. *J. Chem. Phys.* **1998**, *108*, 1452.
(13) Klessinger, M. *Angew. Chem., Int. Ed. Engl.* **1995**, *34*, 549−551.
(14) Yamamoto, N.; Olivucci, M.; Celani, P.; Bernardi, F.; Robb, M. A. *J. Am. Chem. Soc.* **1998**, *120*, 2391−2407 and references therein.
(15) Reguero, M.; Olivucci, M.; Bemardi, F.; Robb, M. A. *J. Am. Chem. Soc.* **1994**, *116*, 2103.
(16) Fang, W. H. *J. Am. Chem. Soc.* **1999**, *121*, 8376.
(17) Jackson, W. N.; Okabe, H. *Adv. Photochem.* **1986**, *13*, 1.
(18) Moore, C. B.; Weisshaar, J. C. *Annu. Rev. Phys. Chem.* **1983**, *34*, 525.
(19) Blom, C. E.; Bauder, A. *Chem. Phys. Lett.* **1982**, *85*, 55.
(20) Hamada, Y.; Nishimura, Y.; Tsumoi, M. *Chem. Phys.* **1985**, *100*, 365.
(21) Shinohara, H.; Nishi, N. *J. Chem. Phys.* **1982**, *77*, 234.
(22) Fujimoto, G. T.; Umstead, M. E.; Lin, M. C. *J. Chem. Phys.* **1985**, *82*, 3042.
(23) Haas, B.-M.; Minton, T. K.; Felder, P.; Huber J. R. *J. Phys. Chem.* **1991**, *95*, 5149.
(24) Ruschin, S.; Bauer, S. H. *J. Phys. Chem.* **1980**, *84*, 3061.
(25) True, N. S.; Bohn, R. K. *J. Phys. Chem.* **1978**, *82*, 478.
(26) Garmona, P.; Moreno, J. *J. Mol. Struct.* **1982**, *82*, 177.
(27) Singleton, D. L.; Paraskevopoulos, G.; Irwin, R. S. *J. Phys. Chem.* **1990**, *94*, 695.
(28) Bolton, K.; Lister, D. G.; Sheridan, J. *J. Chem. Soc., Faraday Trans. 2* **1974**, *70*, 113.
(29) Forman, R. L.; Mackinnon, H. M.; Ritchie, P. D. *J. Chem. Soc. C* **1968**, 2013.
(30) Rosenfeld, R. N.; Weiner, B. *J. Am. Chem. Soc.* **1983**, *105*, 3485.
(31) Rosenfeld, R. N.; Weiner, B. *J Am. Chem. Soc.* **1983**, *105*, 6233.
(32) Arendt, M. F.; Browning, P. W.; Butler, L. J. *J. Chem. Phys.* **1995**, *103*, 5877.
(33) Kitchen, D. C.; Forde, N. R.; Butler, L. J. *J. Phys. Chem. A* **1997**, *101*, 6603.
(34) Osborne, M.; Li, Q.; Smith I. W. M. *Phys. Chem. Chem. Phys.* **1999**, *1*, 1447.
(35) Petty, J. T.; Moore, C. B. *J. Chem. Phys.* **1993**, *99*, 47.
(36) Petty, J. T.; Harrison, J. A.; Moore, C. B. *J. Phys. Chem.* **1993**, *97*, 11194.

10.1021/ja0004579 CCC: $19.00
Published on Web 10/21/2000

mainly on the $CH_2CHCOOH$ photodissociation. Several processes have been proposed as primary dissociation pathways:

$$CH_2CHCOOH + h\nu \rightarrow H_2C{=}CH + HOCO \quad (1)$$

$$\rightarrow H_2C{=}CH_2 + CO_2 \quad (2)$$

$$\rightarrow H_2C{=}CH\,CO + OH \quad (3)$$

$$\rightarrow H_2C{=}CHOH + CO \quad (4)$$

Channel 1 involves the C−C bond cleavage, yielding the radical product, HOCO, which is the intermediate of the OH + CO → H + CO_2 reaction[35,36] that is important in combustion. Some studies[35−37] on the HOCO radical have used reaction 1 to produce this radical. On the basis of the observation of intense infrared fluorescence in the spectral region corresponding to the CO_2 asymmetric stretch after 193 and 248 nm excitation, Rosenfeld and Weiner[31] concluded that decarboxylation, channel 2, is a major process and forms CO_2 excited in the ν_3 vibration. Prompt formation of CO_2 was observed at both wavelengths, suggesting its production in a primary process. Miyoshi and Matsui[37] suggested on the basis of mass spectral evidence that, in addition to the C−C bond fission, reactions 3 and 4 occur after excitation at 193 nm. An extensive study on the photodissociation dynamics of acrylic acid has been performed by Butler and co-workers[32,33] in a crossed laser−molecular beam apparatus. The photofragment velocity distribution measurements indicate that only primary C−C and C−O bond fissions are major photodissociation pathways; molecular decarboxylation and decarbonylation reactions do not occur to a significant extent. The presence of two distinct translation energy distributions for the C−C fission predicts there are two different primary C−C bond fission channels, resulting in the product of HOCO radicals in the ground and first electronically excited states. The photodissociation of acrylic acid by the ultraviolet light from a flashlamp[34] has been investigated by measuring the relative yields of some of the major products by time-resolved infrared absorption using tunable, narrow bond diode lasers. The photodissocation proceeds by at least three competing channels: (1) cleavage of the C−C bond to yield CH_2CH + HOCO, (2) decarboxylation, that is, loss of CO_2 with CH_2CH_2 as coproduct; and (3) or (4) decarbonylation, loss of CO with CH_2-CHOH or CH_2CH + OH as coproducts. The relative yields are found to be [HOCO]:[CO_2]:[CO] = 0.32:0.37:0.31 for the CH_2-CHCOOH photodissociation.

It is evident that the previous experiments do not provide a consistent mechanism of the $CH_2CHCOOH$ photodissociation. To get better understanding of the mechanism involved in acrylic acid photodissociation, high-level ab initio potential energy surfaces are necessary. As far as we know, up to date there are only three theoretical studies on decarboxylation of acrylic and methacrylic acids at the HF level with small basis sets.[38−40] In the present work, the ground- and excited-states potential energy profiles, governing the $CH_2CHCOOH$ dissociation to different products, were traced with the complete active space SCF (CASSCF) approach. The most probable mechanism leading to different photoproducts were determined with the obtained potential energy surfaces and their crossing points.

2. Computational Details

Ab initio molecular orbital methods have been used to investigate the ground- and excited-state potential energy surfaces (PES) of acrylic acid. The stationary points on the ground-state PES are fully optimized with the MP2(FC) and CASSCF energy gradient techniques, where FC denotes the frozen 1s core of oxygen and carbon atoms. The CASSCF gradient technique is used to optimize the stationary points on the potential energy surfaces of excited singlet and triplet states. Since the amount of spin contamination in the reference spin unrestricted wave functions is found to be small, the UMP2 method, in addition to the CASSCF approach, is used to optimize the stationary points on the lowest triplet surface. The points of surface crossing between the four relevant states (S_0, S_1, T_l, and T_2) were determined using the state-averaged CASSCSF method. The nature of critical points is confirmed by an analytical frequency computation. The optimization is terminated when the maximum force and its root-mean-square (rms) are less than 0.00045 hartree/bohr (0.54 kcal mol^{-1} $Å^{-1}$) and 0.0003 hartree/bohr (0.36 kcal mol^{-1} $Å^{-1}$), respectively. After a preliminary search with a 6-31G* basis set, the stationary structures are further optimized with a correlation-consistent atomic natural orbital basis set, cc-pVDZ.[41] All ab initio calculations described here have been performed with the Gaussian 94 or 98 program package.[42]

The choice of active space in the CASSCF computations requires some comment. To describe equilibrium structures of acrylic acid in low-lying electronic states, one needs the π and π^* orbitals of the C=C and C=O fragments and the n orbitals located at the O atoms, that is, eight electrons in six orbitals. For investigating the dissociation processes which involve a break of the C−C or C−O σ bond, the C−C or C−O σ and σ^* orbitals should be included in the active space. This leads to an active space with 10 electrons in eight orbitals, referred to as CAS(10,8), for each of the dissociation processes. Test CASSCF calculations showed that there are at least two orbitals which always have occupancies of two. One of these two orbitals is excluded from the active space. It is not necessary to include the σ orbital in the active space for optimizations of minimum-energy structures. For the C−C or C−O fission, the n orbital of the C=O or OH group is doubly occupied and is discarded. Finally, the CAS(8,7) calculations were performed in the present work.

CASSCF will give a balanced representation of the excited states computed in this work that would not be possible with SCF methods. Thus, the surface topology (minima, transition states and crossings) should be quite reliable. However, the detailed energetics will be sensitive to the inclusion of dynamic correlation. The multireference MP2 (MR-MP2) approach[43] is a very efficient algorithm for treating dynamic correlation, but it is a difficult task, at present, to optimize stationary structures at the MR-MP2 level for acrylic acid. Therefore, energies of some stationary points are calculated with the MR-MP2 approach at the CASSCF optimized structures.

3. Results and Discussion

This section is structured in four subsections. The main features of the ground, triplet and excited singlet surfaces are, respectively, characterized in the first three subsections, while the mechanistic aspects of the $CH_2CHCOOH$ photodissociation are discussed in the last subsection. The energetic data for the critical points on the ground- and excited-state surfaces are given in Tables 1 and 2, respectively. The optimized structures of the critical points are displayed in Figures 1−3. The obtained potential energy profiles are shown in Figure 4a, b, and c.

3.1. The Ground-State Pathways. A. Minimum Energy Structures. Four planar conformers of acrylic acid were

(37) Miyoshi, A.; Matsui, H. *J. Chem. Phys.* **1994**, *100*, 3532.
(38) Fang, W. H.; Fang, D. C.; Liu, R. Z. *Chin. Sci. Bull.* **1993**, *38*, *1965*.
(39) Ruelle, P. *J. Comput. Chem.* **1987**, *8*, 158.
(40) Fang, W. H.; You, X. Z. *Int. J. Quantum Chem.* **1995**, *56*, 43.
(41) Dunning, T. H., Jr. *J. Chem. Phys.* **1989**, *90*, 1007.
(42) Frisch, M. J.; Trucks, G. W.; Schlegel, H. B.; Gill, P. M. W.; Johnson, B. G.; Robb, M. A.; Cheeseman, J. R.; Keith, T.; Petersson, G. A.; Montgomery, J. A.; Raghavachari, K.; Al-Laham, M. A.; Zakrzewski, V. G.; Ortiz, J. V.; Foresman, J. B.; Cioslowski, J.; Stefanov, B. B.; Nanayakkara, A.; Challacombe, M.; Peng, C. Y.; Ayala, P. Y.; Chen, W.; Wong, M. W.; Andres, J. L.; Replogle, E. S.; Gomperts, R.; Martin, R. L.; Fox, D. J.; Binkley, J. S.; Defrees, D. J.; Baker, J.; Stewart, J. P.; Head-Gordon, M.; Gonzalez, C.; Pople, J. A. *Gaussian 94*, revision D.4; Gaussian, Inc.: Pittsburgh, PA, 1995.
(43) McDonall, J. J. W.; Peasley, K.; Robb. M. A. *Chem. Phys. Lett.* **1988**, *148*, 183.

Table 1. MP2/cc-pVDZ Relative Energies (kcal/mol) of the Reactant and Transition States in the Ground State

structures	ΔE^a
$CH_2CHCOOH(S_0)$	0.0
$TS1(S_0)$	59.4
$TS2(S_0)$	65.8
TS3	19.4[b]
$TS4(S_0)$	80.6

[a] Relative energies with zero-point energy correction. [b] Energy relative to $CH_2CHCO(^2A')$.

Table 2. CAS(8,7)cc-pVDZ Relative Energies (kcal/mol) of the Stationary and Crossing Points on the Excited-State Surfaces

structures	ΔE^a
$CH_2CHCOOH(S_0)$	0.0
$CH_2CHCOOH(T_1)$	71.5
$TS1(T_1)$	107.8
$TS2(T_1)$	100.7
$CH_3CHCOO(T_1)$	55.0
$TS3(T_1)$	82.1
$CH_2CHCOOH(T_2)$	86.9
$TS4(T_2)$	114.4
$CH_2CHCOOH(S_1)$	88.6
$TS1(S_1)$	114.8
$CH_2CHCOOH(T_3)$	112.5
S_0/T_1	61.7[b]
S_1/S_0	138.6
S_1/T_1	123.5
T_2/T_1	110.3

[a] Relative energies with zero-point energy correction. [b] The crossing point energies are from state-averaged CASSCF calculations.

identified by an ab initio study at the HF level of theory[44] with a 3-21G basis set. According to the designation in that work, they correspond to s-cis,syn, s-trans,syn, s-cis,anti, and s-trans,anti isomers, respectively. The present calculations confirm the planar s-cis,syn, s-trans,syn, and s-cis,anti conformations to be minimum energy points in the ground-state surface. However, the planar s-trans,anti structure was confirmed to be a first-order saddle point connecting the two equivalent s-trans,anti minima, referred to as $CH_2CHCOOH(S_0)$, in which the carboxyl group rotates about 25° relative to the H_2CCH moiety. Since the dissociation reactions discussed below start from s-trans,anti isomer, and geometric parameters of the different isomers are very close, Figure 1 only shows the structure of s-trans,anti isomer, along with its bond parameters. The isomerization reactions between the different isomers will be discussed separately.

B. The C2−C3 bond fission The C2−C3 bond is of a little double bond character, due to the weak conjugation interaction between the C═C double bond and the carboxyl group. It can be expected that the C2−C3 bond fission does not take place very easily in the ground-state surface. We attempt to optimize a transition state on the ground-state pathway with the CAS-(8,7)/cc-pVDZ approach. The energy gradient ($\partial E/\partial R_{C-C}$) increases gradually to −0.0004 E_h/Å with the growth of the C2−C3 distance till dissociation limit. The saddle point search does not converge, but instead leads to the dissociation products $CH_2CH(^2A')$ and $HOCO(^2A')$. This shows that no transition state exists on the dissociation pathway of $CH_2CHCOOH(S_0)$ into $CH_2CH(^2A')$ and $HOCO(^2A')$. The structure and energy of the separated fragments are determined by a supermolecule calculation. The supermolecule, including both fragments, is optimized with the same basis set and active space as for the optimization of the $CH_2CHCOOH$ molecule. In the resulting structure of the supermolecule, the geometric parameters of CH_2CH and HOCO moieties are the same as those optimized for the corresponding fragments. In this way, the endothermic character of reaction 1 is calculated to be 101.0 kcal/mol at the CAS(8,7)/cc-pVDZ level with the scaled vibrational zero-point energy correction. The calculated value is in good agreement with the experimental estimate of 99.0 and 92.0 kcal/mol cited in refs 34 and 37, and the upper limit of about 100 kcal/mol determined in ref 33.

C. Decarboxylation. There are two possible pathways for acrylic acid to decompose, forming CO_2 product: reaction 1 followed by the HOCO decomposition into CO_2 and H, and the molecular reaction 2. The dissociation process of HOCO to CO_2 and H has been theoretically studied in several groups.[37,45,46] The barrier height of this reaction was estimated to be 39.7 kcal/mol.[37] From the MP2/cc-pVDZ optimized structures and calculated energies here, the barrier height of the HOCO dissociation to H + CO_2 was predicted to be 21.2 kcal/mol with the scaled zero-point energy correction. It is well-known that the HOCO radical is a transient intermediate in the OH + CO → CO_2 + H. The MP2 calculations probably provide a better estimation of the barrier height for the dissociation reaction. Due to high endothermic character of reaction 1, it is a rate-determining step of the ground-state pathway, $CH_2CHCOOH$ → CH_2CH + HOCO → CH_2CH + CO_2 + H.

Reaction 2 can proceed through a 1,3-shift of H6 atom from O5 to C2 atom. A four-centered transition state, $TS1(S_0)$, was found by the CAS(8,7) and MP2 calculations. As shown in Figure 2a, $TS1(S_0)$ has a nonplanar structure with the O4−C3−C2−C1 dihedral angle of about 100°. Upon inspecting the ground-state structure in Figure 1, one can see that an intramolecular rotation takes place prior to the 1,3 H-shift. IRC calculations at the MP2/cc-pVDZ level confirmed that $TS1(S_0)$ is a transition state connecting $CH_2CHCOOH(S_0)$ and CH_2CH_2 + CO_2. The barrier height is calculated to be 59.4 kcal/mol at the MP2/cc-pVDZ level with the scaled zero-point energy correction. Rupple's calculations[39] at the HF/STO-3G level overestimated the barrier by about 40 kcal/mol with respect to the MP2/cc-pVDZ result. Both the present calculations and the experiment agree in predicting that the almost thermoneutral molecular reaction of acrylic acid gives rise to CH_2CH_2 + CO_2.

It is also possible that the H6 atom transfers from O5 to C1 (1,4 H-shift), forming an intermediate of CH_3CHCOO through a five-centered transition state, $TS2(S_0)$ in Figure 2a, and followed by dissociation of CH_3CHCOO into CH_3CH and CO_2. $TS2(S_0)$ was confirmed to be a transition state connecting CH_2-$CHCOOH$ and CH_3CHCOO. The CAS(8,7)/cc-pVDZ calculations show that CH_3CHCOO is of a diradical character, and its ground state is $^3A''$. $CH_3CHCOO(^3A'')$ cannot adiabatically correlate with the ground-state acrylic acid, $CH_2CHCOOH(S_0)$. It can be expected that the surface crossing occurs on the reaction pathway from $CH_2CHCOOH(S_0)$ to $CH_3CHCOO(3A'')$. The structure of the crossing point (S_0/T_1), as shown in Figure 3, was determined by the state-averaged CAS(8,7)/cc-pVDZ calculations, and the energy of S_0/T_1 is 2.2 kcal/mol relative to the $CH_3CHCOO(^3A'')$ minimum. This crossing point in structure is close to $CH_3CHCOO(^3A'')$. With respect to S_0, the height of barrier to 1,4 H-shift is 65.8 kcal/mol, calculated at the MP2/cc-pVDZ level with the scaled zero-point energy correction. The $CH_3CHCOO(^3A'')$ dissociation occurs very easily, due to a barrier of 5.3 kcal/mol on the way to $CH_3CH(^3A'')$ and CO_2.

Considering that the reaction of $CH_2CHCOOH(S_0)$ to CH_3-$CH(^3A'')$ and CO_2 via the intermediate is a multistep and spin-

(44) Loncharich, R. J.; Schwartz, T. R.; Houk, K. N. *J. Am. Chem. Soc.* **1987**, *109*, 14.

(45) Aoyagi, M.; Kato, S. *J. Chem. Phys.* **1988**, *88*, 6409.

(46) Schwartz, G. C.; Fitzcharles, M. S.; Harding, L. B. *Faraday Discuss Chem. Soc.* **1987**, *84*, 359.

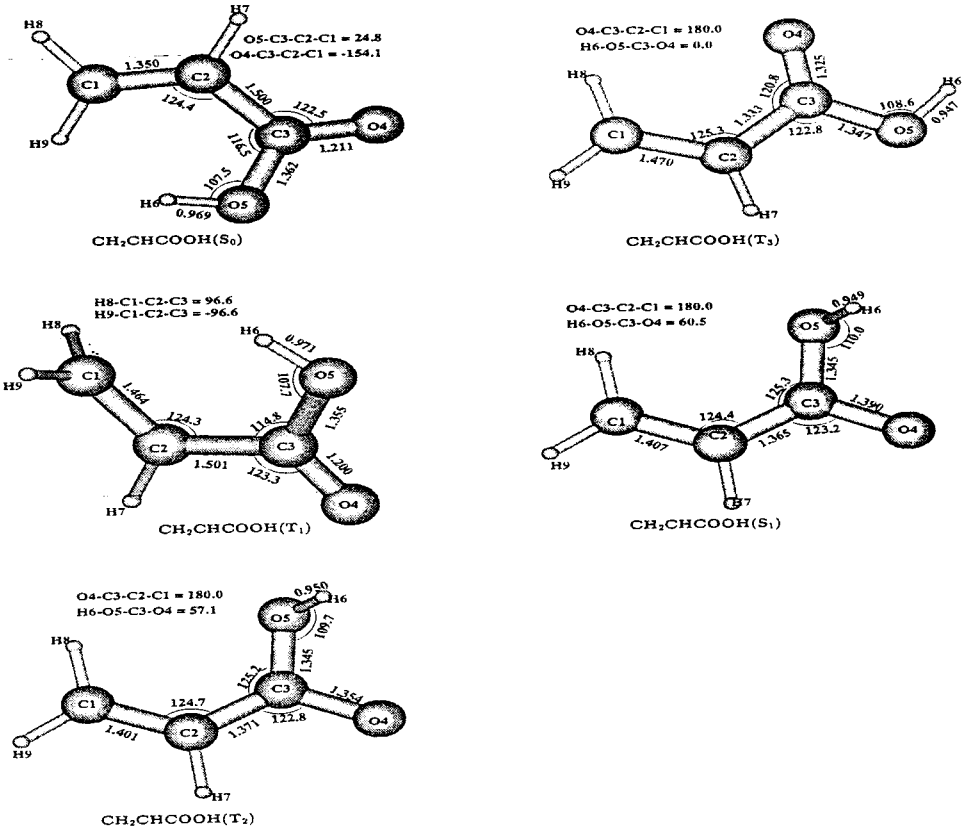

Figure 1. Schematic structures (bond lengths in Å and bond angles in degrees) of acrylic acid in the low-lying electronic states, $CH_2CHCOOH(S_0)$, $CH_2CHCOOH(T_1)$, $CH_2CHCOOH(T_2)$, $CH_2CHCOOH(T_3)$, and $CH_2CHCOOH(S_1)$.

forbidden process, and the barrier of the 1,4 H-shift is a little higher than that of the 1,3 H-shift, the direct decarboxylation via the 1,3 H-shift prevails. As pointed out before, CO_2 can be formed via reaction 1 followed by the HOCO decomposition. Because of high endothermic character of reaction 1, this reaction cannot compete with the direct decarboxylation. Thus, we conclude that in the ground electronic state the direct decarboxylation via the 1,3 H-shift is the most probable channel, forming the product of CO_2. It should be noticed that the barrier of 59.4 kcal/mol for the 1,3 H-shift predicts that the thermo-decarboxylation of acrylic acid proceeds difficultly under normal condition. Early pyrolysis studies[29] showed that acrylic acid is thermostable, and at ~500 °C it breaks down to the extent of ~25% by different reactions, forming CO_2, CO, and other products.

D. Decarbonylation. CO can be generated via two possible pathways. One is the two-step process in which $CH_2CHCOOH$ first dissociates into $CH_2CHCO + OH$, that is, reaction 3, and then the CH_2CHCO radical further decomposes, yielding CH_2-CH and CO. No potential barrier was found above the endothermicity for reaction 3. The reaction is endothermic by 101.0 kcal/mol. It becomes 96.4 kcal/mol with the scaled zero-point energy correction. The standard enthalpy change of this reaction is 104.1 kcal/mol cited in ref 34. The CH_2CHCO radical generated by reaction 3 can dissociate into CH_2CH and CO via a transition state of TS3 shown in Figure 2a. Dissociation of $CH_2CHCO(^2A')$ to $CH_2CH(^2A')$ and $CO(^1\Sigma^+)$ is expected to occur easily. However, the CAS(7,7)/cc-pVDZ calculations predict the barrier height to be 19.4 kcal/mol, including zero-point energy correction. The MR-MP2 calculations give the barrier height of 22.0 kcal/mol. Because of high endothermicity for the first step, reaction 3, the thermo-decarbonylation occurs very difficultly via the above two-step mechanism.

It is possible that the OH group transfers from the C3 to C2 atom, forming CH_2CHOH and CO, namely, reaction 4. A transition state, $TS4(S_0)$ shown in Figure 2a, was found on this pathway. The analysis of the eigenvector corresponding to the negative eigenvalue of the force constant matrix indicates that the reaction vector is principally composed of the C2−C3, O5−C3 bonds and some angles. The reaction vector corresponding to the imaginary frequency ($960i$ cm^{-1}) has been identified as $0.65\ R_{C2-C3} - 0.53\ R_{O5-C3} - 0.29\ A_{C3-O5-C2} + 0.24\ D_{O4-C3-O5-C2}$. It is evident that $TS4(S_0)$ is the transition state connecting $CH_2CHCOOH$ and $CH_2CHOH + CO$. With respect to the zero-point level of $CH_2CHCOOH(S_0)$ the barrier height is 80.6 kcal/mol at the MP2/cc-pVDZ level. In comparison with the two-step process, the one-step decarbonylation proceeds more easily. However, a barrier of 80.6 kcal/mol shows that there is little possibility for the $CH_2CHCOOH(S_0)$ decomposition into $CH_2CHOH + CO$ at room temperature. This is consistent with the high thermostability of acrylic acid.

3.2. The Excited Triplet-State Pathways. A. Minimum Energy Structures. Four minimum energy structures with C_s symmetry exist on the T_1 surface. Only one was shown in Figure 1. The structure of the carboxyl group in the triplet minimum is similar to that in the ground-state equilibrium geometry, while the terminal CH_2 group is nearly perpendicular to the symmetric plane of the molecule, which is different from planar structure of the ground-state molecule. In comparison with the S0 minimum, the C1-C2 bond length is increased by 0.25 Å, while the C2−C3 bond is nearly the same as that in S_0. On the basis of the CAS(8,7)/cc-pVDZ calculated wave functions, a natural orbital analysis shows that two singly occupied orbitals are mainly localized at the C1 and C2 atoms, respectively. It is reasonable to expect that $CH_2CHCOOH(T_1)$ arises from the C=C $\pi \rightarrow \pi^*$ excitation. One electron is initially excited from the

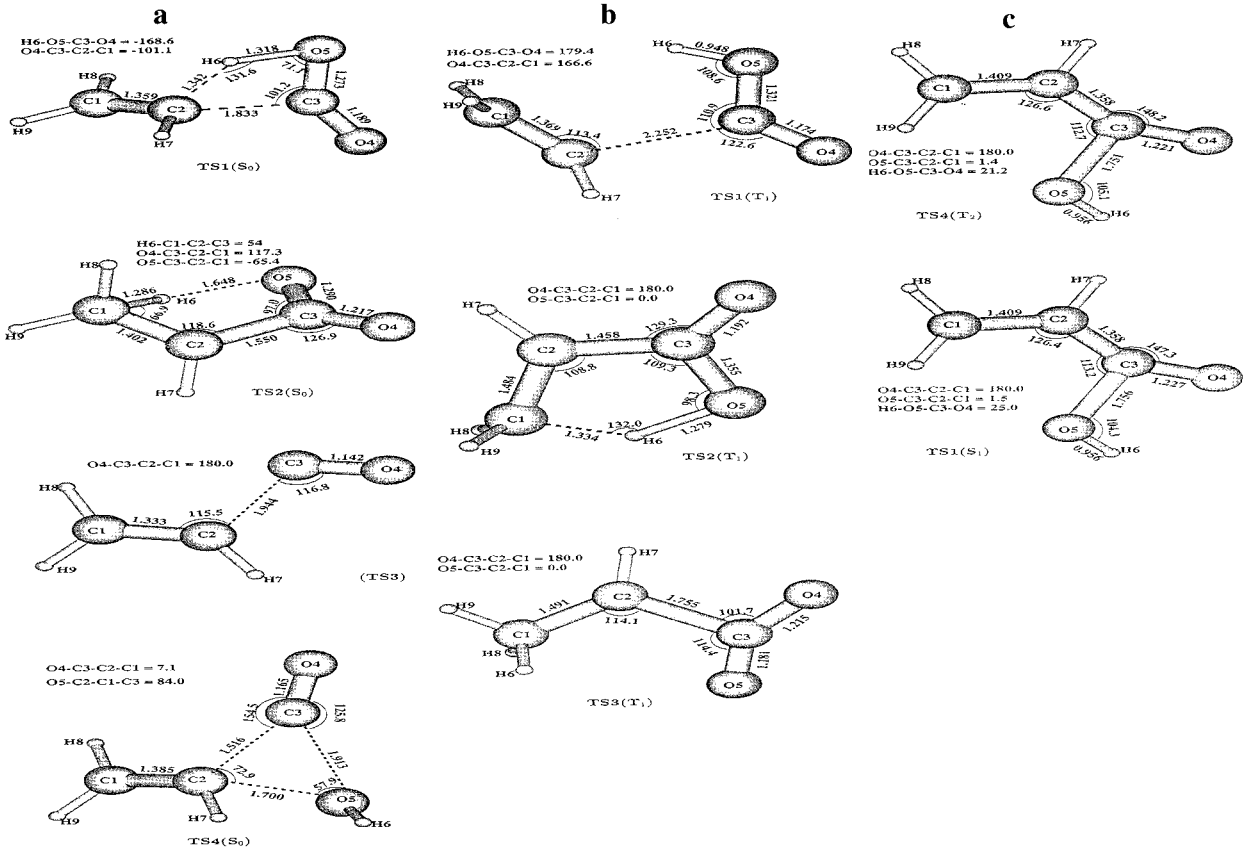

Figure 2. Schematic structures (bond lengths in Å and bond angles in degrees) of the transition states in (a) the ground state (S_0), (b) the lowest triplet state (T_1), and (c) the T_2 and S_1 states.

π to π^* orbital, which makes the C1−C2 π bond nearly broken. In this case, the bond between C1 and C2 atoms is mainly of single bond character, and the terminal CH_2 group can more easily rotate around the C1−C2 bond, leading to the "V-shape" structure[47] like ethylene. A little distortion from the V-shape structure takes place due to an unsymmetric distribution of the atoms with respect to the terminal CH_2 group. The structural character of $CH_2CHCOOH(T_1)$ is very similar to that of CH_2-$CHCHO(T_1)$.[15,16]

With the molecule constrained to be planar, a minimum was found on the triplet surface. The CASSCF wave functions and natural orbital populations show that this constrained minimum is of $^3n\pi^*$ character. However, the constrained triplet minimum is confirmed to be a saddle point upon removal of the symmetry constraint. In the structure of the true triplet minimum, referred to as T_2 in Figure 1, all atoms are actually coplanar, except for H6 which deviates from the molecular plane (the H6−O5−C3−O4 dihedral angle of 57.1°). The C1═C2−C3═O4 backbone in S_0 is changed into Cl−C2═C3−O4 in T_2 with two single electrons in the $2p_z$ orbital of C1 and the n orbital of O4, respectively. It is reasonable to expect that the initial excitation is a local transition from the n orbital to the C═O π^* orbital, which weakens to a large extent the C−O π bond. To stabilize the system, the C2−C3 π bond is formed. The C1−C2═C3−O4 backbone of the $^3n\pi^*$ state for acrylic acid is similar to that for the $^3n\pi^*$ state of acrolein. However, acrolein in $^3n\pi^*$ has a planar structure, which is different from nonplanar CH_2-$CHCOOH(^3n\pi^*)$.

As shown in Figure 1, a planar minimum energy structure, which corresponds to s-trans,syn conformer in the ground state, was found on a triplet surface. On the basis of the CAS(8,7)/cc-pVDZ calculated wave functions, natural orbital analysis shows that in this planar structure the C2−C3 bond has double bond character with two single electrons populated in the $2p_z$ atomic orbitals of the C1 and O4 atoms (the *xy*-plane as the symmetric plane), which is different from that in T_2 where one single electron populates in the n orbital of the O4 atom. The electronic structure of the planar triplet minimum arises from an electronic excitation from the π orbital of the C═C group to the π^* orbital of the C═O bond. After this excitation, the C2−C3 π bond is formed for further stabilizing the system. The planar triplet state is $^3\pi\pi^*$ with a backbone similar to that of T_2. This $^3\pi\pi^*$ state is referred to as T_3, as it is higher in energy than T_1 and T_2. The C1−C2 bond in $T_3(^3\pi\pi^*)$ is 0.07 Å longer than that in T_2, while the C2−C3 and C3−O4 bonds are significantly shortened in $T_3(^3\pi\pi^*)$ with respect to T_2. This structural feature predicts that intramolecular charge-transfer configuration makes a considerable contribution to the electronic structure of $T_3(^3\pi\pi^*)$. The T_3 geometric and electronic structures of acrolein were not determined in the previous studies.[15,16]

B. The C2−C3 Bond Fission. As pointed out before, the C2−C3 bond is mainly of single-bond character in ground state, but it is of double-bond character in the T_2 ($^3n\pi^*$) and T_3 ($^3\pi\pi^*$) states. These indicate that dissociation to CH_2CH + HOCO takes place more difficultly starting from T_2 ($^3n\pi^*$) and $T_3(^3\pi\pi^*)$ than from S_0. Both CH_2CH and HOCO have $^2A'$ ground state. If the two radicals approach to each other in C_s symmetry, they only can correlate with the $^3\pi\pi^*$ ($^3A'$) state, in addition to the ground state ($^1A'$) of $CH_2CHCOOH$. The optimized transition state [TS1(T_1)], as shown in Figure 2b, has C_1 symmetry. In practice, the two radicals do not approach in plane, but nearly perpendicular to each other. The structural feature of TS1(T_1) predicts that it is a transition state connecting $CH_2CHCOOH(T_1)$ and

(47) Davidson, E. R.; Nitzsche. L. E. *J. Am. Chem. Soc.* **1979**, *101*, 6524.

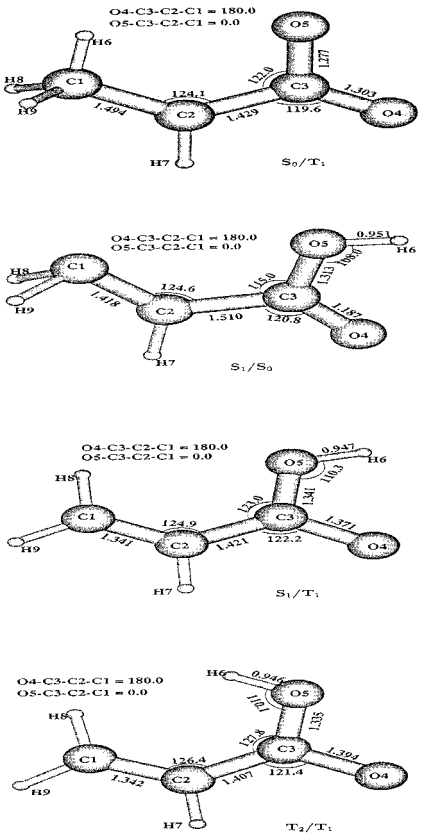

Figure 3. Schematic structures (bond lengths in Å and bond angles in degrees) of the crossing points between the four surfaces (S_0, S_1, T_1, and T_2).

the products of *trans*-HOCO(^{2}A′) + CH_2CH(^{2}A′), which is confirmed by the displacement vectors associated with the imaginary modes of TS1(T_1). With respect to the zero-point level of T_1, the dissociation barrier is calculated to be 36.3 kcal/mol at the CAS(8,7)/cc-pVDZ level. The MR-MP2 calculations stabilize the T_1 minimum, and provide the barrier height of 41.5 kcal/mol. Relatively high barrier arises from the high endothermicity of the dissociation.

C. Decarboxylation. The $T_3(^3\pi\pi^*)$ and $T_2(^3n\pi^*)$ states are planar or nearly planar, there is little possibility that a migration of H6 to C1 occurs within the plane, due to steric effects. Unlike $T_3(^3\pi\pi^*)$ and $T_2(^3n\pi^*)$, the twisted equilibrium geometry of T_1 provides a good opportunity for the H6 migration to Cl atom, which gives us a hint that the photodecarboxylation reaction of acrylic acid may start from $CH_2CHCOOH(T_1)$. The reaction involves a two-step mechanism, namely, isomerization to intermediate [$CH_3CHCOO(^3A'')$] through a transition state [TS2(T_1)], followed by the dissociation into the products $CH_3CH(^3A'')$ + CO_2 via the second transition state [TS3(T_1)]. The CAS(8,7)/cc-pVDZ optimized structures of TS2(T_1) and TS3(T_1) are shown in Figure 2b, along with their structural parameters. In TS2(T_1) the bond between H6 and C1 is partially formed and the H6−O5 bond is partially broken. The analysis of the eigenvector corresponding to the negative eigenvalue of the force constant matrix indicates that the internal coordinate reaction vector is mainly composed of the H6−O5 bond cleavage, the H6−C1 bond formation and a change in the H6−C1−C2, O5−H6−C1 and H6−O5−C3 angles. The reaction vector corresponding to the imaginary frequency (2750.6*i* cm^{-1}) has been identified as 0.76 R_{H6-C5} − 0.59 A_{H6-C1} + 0.16 $A_{H6-C1-C2}$ − 0.10 $A_{H6-O5-C3}$ − 0.10$A_{O5-H6-C1}$. It is obvious that TS2(T_1) is the transition state governing a migration of H6 from O5 to C1. A barrier of 29.2 kcal/mol, calculated at the CAS(8,7)/cc-pVDZ level with the scaled zero-point energy correction, exists on the first step of the triplet decarboxylation pathway. This barrier is reduced to 17.8 kcal/mol by the MR-MP2 calculations. The second step of the triplet pathway involves a breaking of the C2−C3 bond, forming $CH_3CH(^3A'')$ and $CO_2(^1\Sigma_g^+)$. A transition state is optimized and confirmed to be the first saddle point by the CAS(8,7)/cc-pVDZ and UMP2/cc-PVDZ calculations. The best estimation of the barrier height is 5.3 kcal/mol, which is shown in Figure 4b. It is evident that the isomerization to $CH_3CHCOO(^3A'')$ is the rate-determining step of the triplet decarboxylation of acrylic acid. It has been found[48] that triplet methylcarbene does not exist as a stable species. It will undergo intersystem crossing to the singlet surface and immediately transform to the ground-state ethylene.

D. Decarbonylation. All attempts to optimize a transition state for one-step decarbonylation on the triplet surface were unsuccessful, as the optimizations invariably collapsed to TS4(T_2) in Figure 2c, a transition state for the C3−O5 bond cleavage on the T_2 surface. Thus, the $CH_2CHCOOH$ decarbonylation occurs on the T_2 surface via a two-step mechanism. The first step involves a break of the C3−O5 bond, yielding CH_2CHCO and OH in their electronic ground state. Then, the formed CH_2CHCO radical dissociates into CH_2CH and CO along the ground-state pathway, which has been discussed before.

Although geometry optimization was carried out without any symmetric constraint, in the resulting structure of TS4(T_2) all atoms are actually coplanar, except the H6 atom which significantly deviates from the molecular plane (H6−O5−C3−O4 of about 20°), which is similar to the situation in $T_2(^3n\pi^*)$. Since the C3−O5 bond is nearly broken in TS4(T_2), the C3−O4 bond is shortened with respect to that in $T_2(^3n\pi^*)$. The similarity in structures of $T_2(^3n\pi^*)$ and TS4(T_2) predicts that TS4(T_2) is the transition state governing the $CH_2CHCOOH(^3n\pi^*)$ dissociation into $CH_2CHCO(^2A'$ and $OH(^2\Pi)$ along the T_2 pathway. This conclusion has been confirmed by the IRC calculations. The ground-state OH and CH_2CHCO radicals are of $^2\Pi$ and $^2A'$ symmetry, respectively. When the two radicals approach each other in C_1 or C_s symmetry, they can adiabatically correlate with the two lowest triplet states of acrylic acid, in addition to singlet states. With respect to zero-point level of $T_2(^3n\pi^*)$, the barrier to the dissociation is 27.5 and 18.6 kcal/mol at the CAS(8,7)/cc-pVDZ and UMP2/cc-pVDZ levels of theory, respectively.

3.3. The Excited Singlet-State Pathways. A. Minimum-Energy Structure. Unlike the ground and the triplet states, only one minimum-energy structure was found on the first excited singlet surface (S_1). The geometric parameters of the S_1 minimum are given in Figure 1. All atoms in the S_1 minimum are actually coplanar, except the H6 atom that deviates from the molecular plane (the H6−O5-C3−O4 dihedral angle of 60.5°). A comparison shows that the S_1 minimum in structure is very similar to $T_2(^3n\pi^*)$. Natural orbital populations and the CASSCF wave functions of the S_1 minimum are almost the same as those for $T_2(^3n\pi^*)$. All of these show that this minimum should be of $^1n\pi^*$ character. It is referred to as $S_1(^1n\pi^*)$. It has been found[15,16] that the S_1 acrolein has a planar structure. The difference in structure between the S_1 acrolein and acrylic acid is induced by replacing the H atom with the OH group.

The bond between the C2 and C3 atoms is mainly of double bond character in $S_1(^1n\pi^*)$, more energy is required in order to

(48) Ha, T. K.; Nguyen, M. T.; Vanquickenbome, L. G. *Chem. Phys. Lett.* **1982**, *92*, 459.

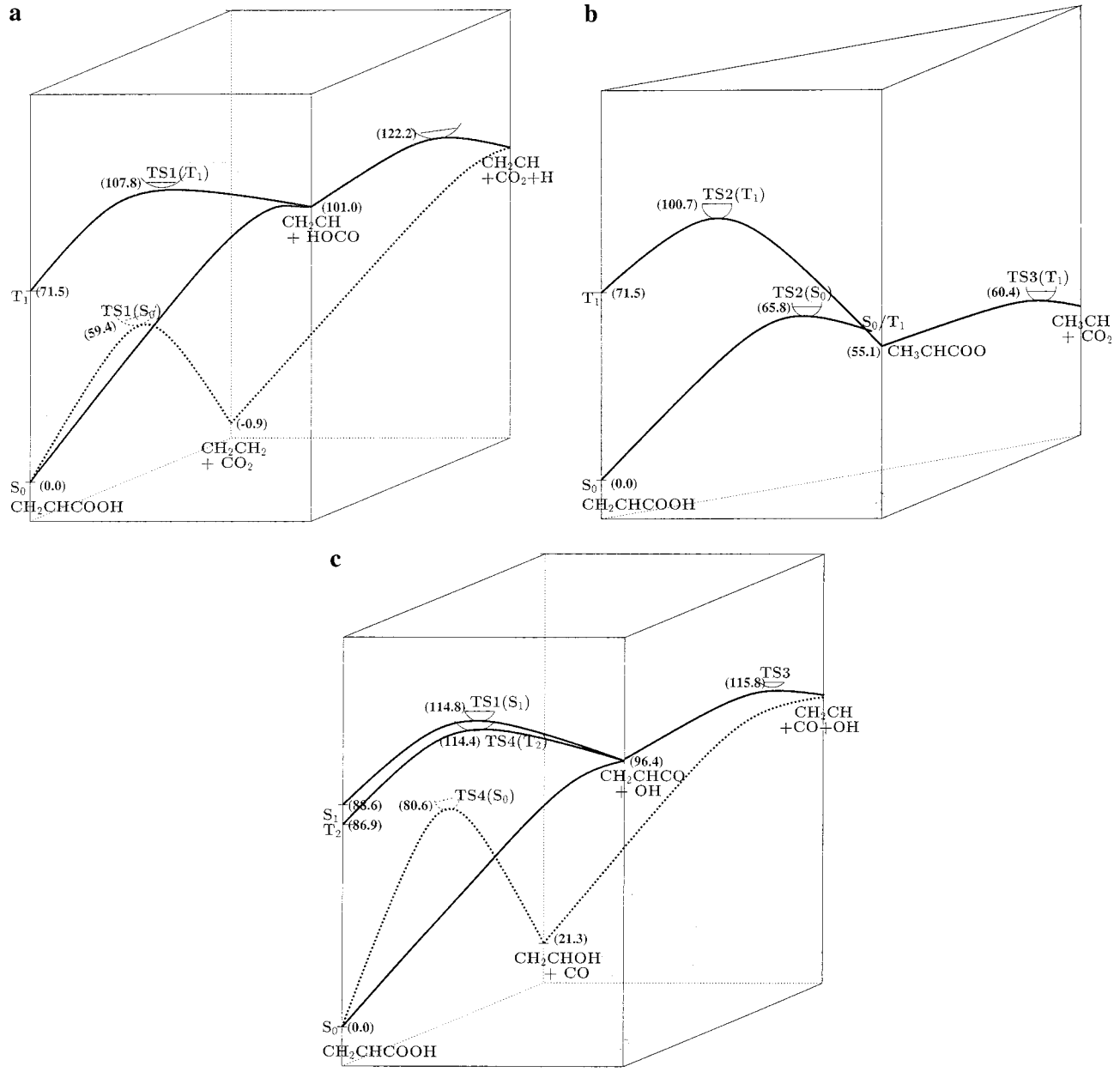

Figure 4. Schematic potential energy profiles of the different electronic states (relative energies in kcal/mol). (a) $CH_2CHCOOH \rightarrow CH_2CH_2 + CO_2$ and $CH_2CHCOOH \rightarrow CH_2CH + COOH \rightarrow CH_2CH + CO_2 + H$; (b) $CH_2CHCOOH \rightarrow CH_3CHCOO \rightarrow CH_3CH + CO_2$; (c) $CH_2CHCOOH \rightarrow CH_2CHOH + CO$ and $CH_2CHCOOH \rightarrow CH_2CHCO + OH \rightarrow CH_2CH + CO + OH$.

yield CH_2CH and HOCO through the C2−C3 bond cleavage, as compared with the reaction starting from the ground state. The S_1 potential energy profile of the $CH_2CHCOOH$ dissociation to $CH_2CH(^2A')$ and $HOCO(^2A'')$ was stepwise optimized at each fixed C2−C3 separation. The barrier height was estimated to be 65 kcal/mol at the C2−C3 separation of 2.4 Å. When the $CH_2CH(^2A'$ and $HOCO(^2A')$ radicals approach to each other in C_1 or C_s symmetry, they only can correlate adiabatically with acrylic acid in the ground state. The adiabatic dissociation of $CH_2CHCOOH$ on the S_1 surface will lead to formation of HOCO in its excited electronic state ($^2A''$). The CAS(7,7)/cc-pVDZ calculations give the $^2A' \rightarrow {}^2A''$ adiabatic exciation energy of about 60 kcal/mol for HOCO, which is mainly responsible for a high barrier on the S_1 pathway to $CH_2CH(^2A')$ and $HOCO(^2A'')$. This process is not in competitive with the S_1 dissociation to $CH_2CHCO(^2A)$ and $OH(^2\Pi)$, which will be discussed below. In addition, One-step decarboxylation and decarbonylation involve breaking and formation of several bonds simultaneously, these processes take place very difficultly on the S_1 surface. It is reasonable to expect that reactions 1, 2, and 4 proceed along the S_1 pathway with less possibility.

B. The C3−O5 Bond Fission. In addition to correlating with the ground and two lowest triplet states of acrylic acid, the $CH_2CHCO(^2A')$ and $OH(^2\Pi)$ fragments can correlate adiabatically with the $CH_2CHCOOH$ molecules in the S_1 state. A nonplanar saddle point, $TS1(S_1)$ shown in Figure 2c, was found on the S_1 surface. $TS1(S_1)$ in structure is very similar to $TS4(T_2)$ which was confirmed to be the transition state governing the $CH_2CHCOOH(^3n\pi^*)$ dissociation to $CH_2CHCO(^2A')$ and $OH(^2\Pi)$. It is evident that $TSl(S_1)$ should be the transition state connecting the $CH_2CHCOOH(^1n\pi^*)$ and $H_2CCHCO(^2A') + OH(^2\Pi)$. Including vibrational zero-point energy correction, the $CH_2CHCOOH(^1n\pi^*)$ dissociation to $CH_2CHCO(^2A')$ and $OH(^2\Pi)$ has a barrier height of 26.2 kcal/mol, obtained with CAS(8,7)/cc-pVDZ calculations. The potential energy profiles was shown in Figure 4.

3.4. Mechanistic Aspects. Photodissociative reactions of acrylic acid are probably nonadiabatic, the reactions start from an excited-state surface and may proceed along the ground, lowest excited singlet, or triplet pathway. Thus, intersection points of surfaces play an important role in describing mechanistic photodissociation of acrylic acid. The minimum energy crossing points between the four surfaces (S_0, S_1, T_1, and T_2), labeled S_0/T_1 S_1/S_0, S_1/T_1, and T_2/T_1 in Figure 3, were optimized at the state-averaged CAS(8,7)/cc-pVDZ level. The resulting structures and energies are given in Figure 3 and Table 2, respectively.

The structural parameters of the carboxyl group in S_1/S_0 are similar to those in the ground state, while the C1−C2 bond length in S_1/S_0 is closer to that in $S_1(^1n\pi^*)$. In addition, the C2−C3 bond length in S_1/S_0 is 1.510 Å, close to the corresponding value of 1.500 Å in the S_0 structure. The S_1/S_0 contains more character of the S_0 minimum than that of S_1 minimum. The S_1/S_0 point lies 47.4 kcal/mol in energy above the S_1 minimum. The S_1/T_1 point has a planar structure. Its geometric parameters are close to those in the S_1 minimum. As pointed out before, the S_1 and T_1 states are of the $^1n\pi^*$ and $^3\pi\pi^*$ character, respectively. The intersystem crossing (ISC) from S_1 to T_1 is expected to occur with a high efficiency.[49] The S_1/T_1 point is 32.3 kcal/mol in energy higher than the S_1 minimum, but 15.1 kcal/mol lower than the S_1/S_0 point. The ISC from S_1 to T_1 takes place more easily than the internal conversion to S_0.

For acrolein, the S_1/S_0 point has a perpendicular structure with the terminal CH_2 group twisted by 90°, while the S_1/T_1 structure is planar. The structural features of the crossing points for acrolein are similar to those for acrylic acid. The S_1/S_0 and S_1/T_1 points are 15.0 and 4.0 kcal/mol in energy above the S_1 minimum for acrolein. The energy order of the S_1/S_0, S_1/T_1, and minimum points for acrolein is consistent with that of the corresponding points for acrylic acid. Relative to the S_1 minimum, however, the S_1/S_0 and S_1/T_1 points are lower in energy for acrolein than for acrylic acid. As a result, internal conversion (IC) from S_1 to S_0 can occur for acrolein, but for acrylic acid, the IC cannot compete with direct dissociation on the S_1 surface, which is discussed below.

An attempt to optimize the S_1/T_2 crossing point was unsuccessful. Since both S_1 and T_2 originate from the same electronic configuration ($n^1\pi^{*1}$), there is less possibility that the S_1/T_2 intersystem crossing occurs,[49] as compared with the ISC from S_1 to T_1. Therefore the S_1/T_2 ISC will not play an important role in the processes of the $CH_2CHCOOH$ photodissociation. As shown in Figure 3, the T_2/T_1 conical crossing point has a planar structure, and its backbone structure is very similar to that in the T_2 minimum. The energy of the T_2/T_1 point is 14.3 kcal/mol higher than that of the T_2 minimum. The internal conversion from T_2 to T_1 should have a high efficiency. A planar T_2/T_1 crossing point was also found for acrolein.[15]

Irradiation of acrylic acid at 248 and 193 nm makes the system populate in the $^1n\pi^*$ and $^1\pi\pi^*$ states, respectively. The corresponding vertical excitation energy is about 115 and 148 kcal/mol, respectively. Since $^1\pi\pi^*$ is a high excited electronic state with the same symmetry as the ground state, at present, the $^1\pi\pi^*$ minimum is difficult to treat computationally. The $CH_2CHCOOH$ molecules in the $^1\pi\pi^*$ state correlate adiabatically with high excited electronic state of the fragments, which is nearly inaccessible in energy even photoexciattion at 193 nm. Experimentally, it has been found that the $CH_2CHCOOH$ photodissociation at 199 nm does not proceed through a single dissociation mechanism.[32] Rather, it would seem that excitation is initially to a predissociative state from which the dissociation channels are made accessible. Therefore, the adiabatic dissociation starting from $^1\pi\pi^*$ state is not considered in the present work.

When the $CH_2CHCOOH$ molecules are excited to the $^1\pi\pi^*$ state, internal conversion to S_1 ($^1n\pi^*$) occur with a high efficiency. This is supported by the fact that photofragmentation at 248 and 193 nm gave the same fragments.[31] From the S_1 state, the ground-state fragments of $OH(^2\Pi)$ and CH_2CHCO ($^2A'$) are formed with a barrier of 26.2 kcal/mol. This barrier is 3.8 and 18.9 kcal/mol in energy lower than the S_1/T_1 and S_1/S_0 points, respectively. Thus, the $CH_2CHCOOH$ molecules relaxing to the S_1 state or populated in the S_1 state by photoexcitation at 248 nm dissociate directly on the S_1 surface, forming $OH(^2\Pi)$ and CH_2CHCO ($^2A'$). The intersystem crossing from S_l to T_1 is another pathway for the $CH_2CHCOOH(S_1)$ deactivation, which can compete with the direct dissociation on the S_1 surface. Once the $CH_2CHCOOH$ molecules relax to the T_1 state, $CH_2CHCOOH(T_1)$ will isomerize to $CH_3CHCOO(T_1)$, followed by the $CH_3CHCOO(T_1)$ dissociation into $CH_3CH(^3A'')$ and $CO_2(^1\Sigma^+)$. The MR-MP2 calculations predict that the barrier to the dissociation of $CH_2CHCOOH(T_1)$ into $CH_2CH(^2A')$ and $COOH(^2A')$ is higher than that of the isomerization. However, the T_1 decarboxylation is a two-step process, the T_1 dissociation may compete with the decarboxylation on the T_1 surface.

Although the $^1\pi\pi^*/T_2$ crossing point is difficult to determine at present, the ISC from $^1\pi\pi^*$ to T_2 is expected to take place with an efficiency comparable to the S_1/T_1 intersystem crossing.[49] After the system relaxes to the T_2 state, the $CH_2CHCOOH(T_2)$ dissociation to CH_2CHCO ($^2A'$) and $OH(^2\Pi)$ can occur on the T_2 surface. The barrier energy on this pathway is nearly the same as that of the corresponding reaction on the S_1 surface. Thus, the $^1\pi\pi^*/T_2$ ISC followed by the direct dissociation on the T_2 surface is an important pathway for formation of CH_2CHCO ($^2A'$) and $OH(^2\Pi)$. As shown in Figure 3, the T_2/T_1 crossing point has a planar structure. Its backbone structure is close to that of the T_2 minimum. The structural similarity between the T_2/T_1 and T_2 predicts the internal conversion from T_2 to T_1 occurs very easily. Again, a pair competitive pathways, the isomerization to $CH_3CHCOO(T_1)$ and dissociation to $CH_2CH(^2A')$ and $COOH(^2A')$, can occur on the T_1 surface.

The direct dissociation takes place easily on the S_1 surface, while the internal conversion from S_1 to S_0 cannot compete with the direct dissociation. Therefore, the $CH_2CHCOOH$ photodissociation at 248 nm proceeds mainly along the S_1 pathway. However, internal conversion from $^1\pi\pi^*$ to S_0 can occur with a considerable efficiency. The $CH_2CHCOOH$ molecules populated in $^1\pi\pi^*$ by photoexcitation at 193 nm which return to the ground state are left with sufficient internal energy to overcome the barriers on the ground-state pathways, forming $CH_2CH_2 + CO_2$, $CO + CH_2CHOH$ or $CH_2CH + HOCO$. However, the direct decarboxylation on the So surface is favorable in energy.

4. Summary

In the present paper, ab initio studies have been performed in order to get better understanding of the $CH_2CHCOOH$ photodissociation. The most probable mechanism leading to different products is characterized on the basis of the obtained potential energy profiles and the crossing points of the S_0, S_1, T_1, and T_2 surfaces. Absorption of 193-nm light corresponds to 148 kcal/mol excitation in $CH_2CHCOOH$, the molecules are populated on the $^1\pi\pi^*$ state. From this state, the system can

(49) Turro, N. J. *Modern Molecular Photochemistry*; Benjamin /Cummings: Menlo, Park, CA, 1978.

decay through three radiationless routes, internal conversion to S_0, to S_1 and intersystem crossing to T_2. The direct dissociation to $CH_2CHCO(^2A')$ and $OH(^2\Pi)$ occurs on the T_2 or S_1 surface with high efficiency. This is the most probable pathway for the formation of $CH_2CHCO(^2A')$ and $OH(^2\Pi)$. The fragments of $CH_2CH(^2A'')$ and $HOCO(^2A')$ are formed principally via relaxation to T_1 followed by the dissociation on the T_1 surface. The IC to S_0 followed by the ground-state dissociation can lead to formation of $CH_2CH(^2A')$ and $HOCO(^2A')$, but the dissociation is not in competition with the decarboxylation and decarbonylation in the ground-state surface.

The $CH_2CHCOOH$ molecules in the $^1\pi\pi$ state which return to the ground state have sufficient internal energy to overcome the barrier on the way to $CH_2CH_2 + CO_2$ or to $CH_2CHOH + CO$, which are main pathways for formation of CO_2 and CO, respectively. But the decarboxylation is a little easier than the decarbonylation. This is consistent with the relative yields of 0.37 and 0.31 for CO_2 and CO, respectively. It should be pointed out that decarboxylation on the T_1 surface is another channel of generating CO_2.

Acknowledgment. The project has been supported by the National Natural Science Foundation of China (Grant Nos. 29673007 and 29873008). One of the authors (W.H.F.) is grateful for Alexander von Humboldt Foundation of Germany for the donation of an IBM work-station.

Supporting Information Available: Vibrational zero-point energies and energies of the investigated stationary point structures (PDF). This material is available free of charge via the Internet at http://pubs.acs.org.

JA0004579